Contents lists available at ScienceDirect

Chemical Engineering Research and Design

journal homepage: www.elsevier.com/locate/cherd

Poly(arylene ether sulfone) copolymers as binders for capacitive deionization activated carbon electrodes

Benjamin M. Asquith[a,b], *Jochen Meier-Haack*[b], *Bradley P. Ladewig*[a,c,*]

[a] *Department of Chemical Engineering, Monash University, Melbourne 3800, VIC, Australia*
[b] *Leibniz Institute of Polymer Research Dresden, Hohe Strasse 6, 01069 Dresden, Germany*
[c] *Department of Chemical Engineering, Imperial College London, Exhibition Road, London SW7 2AZ, United Kingdom*

ARTICLE INFO

Article history:
Received 28 January 2015
Received in revised form 8 July 2015
Accepted 21 July 2015
Available online 28 July 2015

Keywords:
Capacitive deionization
Electrochemical impedance spectroscopy
Cyclic voltammetry
Wettability
copolymers

ABSTRACT

Activated carbon electrodes for capacitive deionization (CDI) have been prepared using poly(arylene ether sulfone) random copolymers as binders. Due to the reduced mechanical strength and enhanced swelling of the polymers compared with PVDF binder, a 15 wt.% composition was found to be required to adequately bind the carbon particles. The hydrophilic nature of the polymers increased the wettability of the electrodes, however CV and EIS testing revealed a loss in capacitance compared with electrodes prepared with PVDF. This is thought to have been a result of polymer swelling, which reduced particle contact and hence charge transfer pathways within the carbon electrodes. As a result, poor micropore double layer formation was observed. Promisingly, EIS testing showed low charging resistance compared with electrodes prepared with PVDF, indicating the potential for hydrophilic polymers to be used as binders in CDI electrodes if charge transfer pathways between carbon particles can be maintained.

1. Introduction

Capacitive deionization (CDI) is a developing desalination technology that can be used for the highly efficient desalination of brackish water (El-Deen et al., 2014; Kim and Choi, 2010; Li and Zou, 2011; Mossad et al., 2013; Xu et al., 2008; Zhang et al., 2013), the production of ultra pure water (Jande and Kim, 2014; Jande et al., 2013; Lee and Choi, 2012), water softening and the removal of other charged impurities from water streams (Farmer, 1995). It is an electrosorption process that relies on the formation of an electrical double layer on a porous, polarizable electrode. When a potential is applied across two porous electrodes, a build up of charge in the electrodes is created. As water is passed between them, the charge is balanced by the ionic charge of dissolved components being removed from the solution (i.e. anions and cations are adsorbed onto the electrode surface). Once the electrodes become saturated with ions, the electrical potential is removed and ions are released back into solution, creating a concentrated waste stream. A simplified representation of CDI adsorption and desorption cycles is shown in Fig. 1.

The high efficiency of CDI for brackish water desalination is a result of the direct removal of ions from the water, compared with the removal of fresh water from a more concentrated feed solution in thermal or pressure driven desalination processes (such as multi-stage flash distillation or reverse osmosis) (Mossad and Zou, 2013). As a desalination process that works most effectively for low salinity water, improvements in the efficiency of CDI will help improve the options available for the desalination of inland brackish water.

Despite activated carbon being widely studied as a material for CDI electrodes (Bouhadana et al., 2011; Choi, 2010;

* *Corresponding author at:* Imperial College London, Department of Chemical Engineering, Exhibition Road, London SW7 2AZ, United Kingdom. Tel.: +44 20 7594 8977.
E-mail address: b.ladewig@imperial.ac.uk (B.P. Ladewig).
http://dx.doi.org/10.1016/j.cherd.2015.07.020
0263-8762/

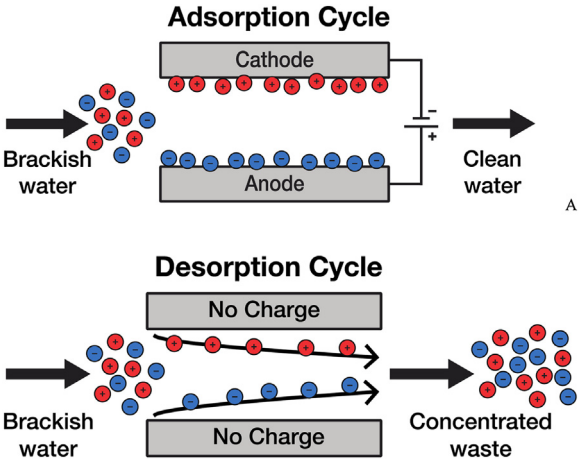

Fig. 1 – Schematic representation of the CDI process.

Hou and Huang, 2013; Hou et al., 2012; Huang et al., 2012; Mossad and Zou, 2012; Porada et al., 2012; Ryoo et al., 2003; Ryoo and Seo, 2003; Villar et al., 2010; Wang et al., 2012; Wang et al., 2013), one of the drawbacks associated with its use is the requirement for a polymeric binder. Typically hydrophobic polymers such as poly(tetrafluoroethylene) (PTFE) (Chang et al., 2012; Lee et al., 2009) or poly(vinylidene fluoride) (PVDF) (Zhang et al., 2012) are used to bind activated carbon powder. However, these binders can hinder ion access to the pores and reduce the wettability of an electrode (Park and Choi, 2010; Park et al., 2011), reducing adsorption capacity, may be susceptible to chemical attack, and yield electrodes with poor electrical conductivity. While increasing the binder content increases mechanical strength, this also serves to reduce electrode capacitance and adsorption efficiency. An optimal amount of binder is therefore required to allow adequate binding strength while limiting the drop off in capacitance and efficiency, with typical binder content in the range 5–15 wt.%.

An alternative method to improve electrode performance is to increase hydrophilicity using fixed charges in the binder. Using this approach, Park et al. (2011) fabricated activated carbon electrodes with a poly(vinyl alcohol) (PVA) binder crosslinked with glutaric acid (GA). As PVA is a water-soluble polymer, crosslinking with GA was used to prevent PVA dissolution. Greater degrees of crosslinking were seen to reduce both the swelling of the PVA polymer and resistance, and greater concentrations of GA improved electrode sorption capacity. Furthermore, unreacted carboxylic acid groups on the GA molecule gave the electrodes a negative surface potential, yielding cation-selective electrodes that could be used as cathodes. When used in a CDI system, the adsorption efficiency of desalting a 200 mg/L NaCl solution was found to be 85%. In contrast, similar electrodes fabricated from activated carbon and PVDF as a binder, were found to have a CDI salt removal efficiency of only 78% (Choi, 2010). Enhanced CDI performance has also been shown by Lee et al. (Lee et al., 2009) through the incorporation of an ion exchange resin into an activated carbon powder electrode.

Similarly, the incorporation of fixed charges has been shown to work with carbon nanotubes. Nie et al. (2012) prepared composite carbon nanotube-polyacrylic acid film electrodes using an electrophoretic deposition method, which showed enhanced desalination performance over both carbon nanotube electrodes and carbon nanotube electrodes combined with a cation exchange membrane. In this instance, the polyacrylic acid acts both as a binder to hold the CNTs and a cation exchange membrane.

In this work, the use of sulfonated poly(arylene ether sulfone) copolymers as a binder material for activated carbon electrodes was investigated. The three key areas of study were the mechanical properties of the polymers, the mechanical properties of carbon electrodes prepared with these polymers, and the electrochemical performance of the electrodes when tested using CV and EIS.

2. Experimental

2.1. Materials

4,4′-Difluorodiphenyl sulfone (DFDPhS) was purchased from FuMA-Tech GmbH (Germany) and was purified by vacuum distillation. 4,4′-Dihydroxydiphenyl sulfone (DHDPhS) was obtained from Aldrich (Germany). 2,5-diphenylhydroquinone (DPhHQ) had been prepared as per the procedure described by Vogel et al. (2011). Calcium carbonate was purchased from Merck (Germany). Potassium carbonate was purchased from Fluka (Germany), and concentrated sulfuric acid (min. 96%) was obtained from Acros (Belgium). Anhydrous NMP, PVDF and activated carbon purchased from Sigma Aldrich (Australia), and carbon black was obtained from TIMCAL Graphite and Carbon (Switzerland). Both the activated charcoal and carbon black were dried for 24 h at 150 °C to remove any moisture or other volatiles. The BET specific surface areas of the activated carbon and carbon black were 1039 and 65 m^2/g, respectively.

2.2. Random copolymer preparation

Three random copolymers (RCP 1–3) were synthesized using the silyl-method as per the procedure previously described (Asquith et al., 2014, 2013; Vogel et al., 2011). The ratio of the monomers in the random copolymers was varied such that the monomer ratio of DPhHQ to DHDPhS was 6:4 for RCP 1, 5:5 for RCP 2 and 4:6 for RCP 3. All polymers were sulfonated using concentrated sulfuric acid (96–98%). The molecular structure of the random copolymers can be seen in Fig. 2.

2.3. Carbon electrode preparation

Carbon electrodes were fabricated from activated charcoal, carbon black and either PVDF or a random copolymer. Electrodes were prepared by first dissolving either PVDF or one of the sulfonated random copolymers in NMP, with the concentration being approximately 5 wt.%. Once fully dissolved carbon black was added and the solution was mixed for several hours. Activated charcoal was then added to form a thick slurry, which was stirred for 12–16 h to ensure an even distribution of carbon black and carbon particles in the PVDF solution. The slurry was coated onto graphite sheets to a thickness of 200 μm using a doctor blade then dried under vacuum initially for 2 h at 40 °C, followed by 12 h at 60 °C and finally 24 h at 100 °C.

2.4. Binder properties

Molecular weights of the sulfonated polymers were obtained from GPC measurements on a Knauer GPC equipped with

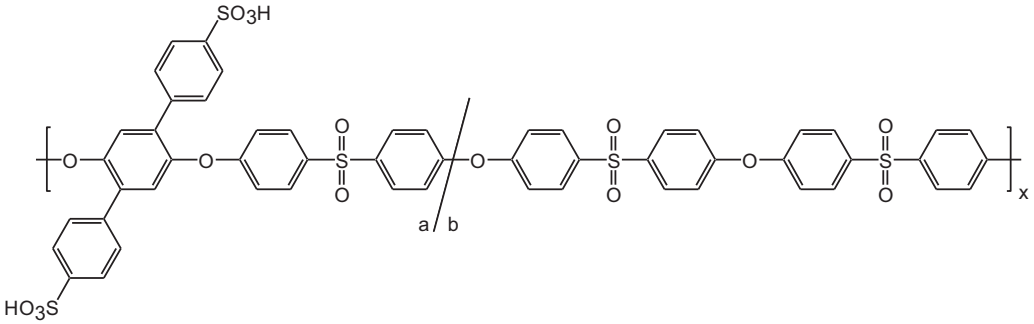

Fig. 2 – Repeating unit of the random copolymer. RCP 1: $a = 6$, $b = 4$; RCP 2: $a = 5$, $b = 5$; RCP 3: $a = 4$, $b = 6$.

Zorbax PSM Trimodal S columns and a RI detector. A mixture of DMAc with 2 vol.% water and 3 g/L LiCl was used as eluent. Thermogravimetric Analysis (TGA) was performed using an EXSTAR TG/DTA 6300 (Seiko Instruments Inc.) under an argon purge at a flow rate of 120 mL/min. The temperature range was 50–700 °C with a heating rate of 10 °C/min.

Tensile testing, contact angle and water uptake measurements were made using membranes fabricated from the polymers. Membranes were prepared by dissolving the sulfonated polymers in NMP. The solutions were cast onto glass and dried under vacuum for 2 h at 60 °C, then for a further 24 h at 80 °C. Membrane samples were removed from the glass using deionized water and thoroughly rinsed with deionized water before soaking for 24 h in 1 M NaCl. The membranes were finally stored in deionized water at room temperature before use. Tensile testing was performed using an Instron Model 5848 MicroTester with a 100 N load cell. Water uptake was measured by first drying membrane pieces at 80 °C under vacuum until constant weight was reached. After soaking the pieces in water at room temperature for 24 h, they were removed, excess water was gently wiped with a tissue and the pieces were immediately weighed. The water uptake (WU) was calculated using the following equation:

$$\mathrm{WU} = \frac{m_{\mathrm{wet}} - m_{\mathrm{dry}}}{m_{\mathrm{dry}}} \quad (1)$$

where m_{wet} is the weight of the swollen membrane and m_{dry} is the weight of the dry membrane.

2.5. *Electrode properties*

Contact angle measurements of electrodes were made with a Dataphysics OCA 15EC Measuring Instrument using the sessile drop method. SEM images were obtained using a Nova NanoSEM 450 with an acceleration voltage of 5 kV using the secondary imaging mode. All samples were coated with iridium prior to imaging. CV and EIS experiments were performed using a Biologic VSP potentiostat connected to a three-electrode electrochemical cell. The working electrode was the carbon material to be tested with an exposed surface area of 0.785 cm^2, the reference electrode was a saturated KCl Ag/AgCl electrode, and the counter electrode was a mesh platinum electrode. EIS was performed using the same cell over the frequency range 10 mHz to 1 MHz, with an applied voltage amplitude of 10 mV. The electrolyte for all electrochemical tests was 0.5 M NaCl.

Table 1 – Contact angle and water uptake of membranes cast from random copolymers or PVDF.

Polymer	Contact angle (°)		Water uptake* (%)
	Initial	Final	
RCP 1	51.8	30.3	49.9
RCP 2	52.1	38.2	35.7
RCP 3	62.3	46.1	25.9
PVDF	81.8	81.3	0.95

* Water uptake measured in the Na^+ form for RCP 1–3.

3. Results and discussion

3.1. *Mechanical properties of binder materials*

3.1.1. *Water uptake and contact angle*

The water uptake and contact angle of membranes cast from the random copolymers and PVDF can be seen in Table 1, where the initial and final contact angles were measured at $t = 0$ s and $t = 54$ s. The contact angle of these polymers is also presented in Fig. 3.

The hydrophobicity of PVDF compared with the random copolymers is clearly seen in both Table 1 and Fig. 2, with a contact angle of 81.8° and a water uptake of 0.95%. By way of comparison, the cation exchange copolymers have much greater swelling properties, ranging from 26.4–49.9% in the Na^+ form. Unlike the dynamic contact angles of the copolymers seen in Fig. 2, the contact angle of the PVDF remained relatively constant over a period of one minute. In terms of usefulness as a binder material, the increased hydrophilicity of the random copolymers is a double-edged sword; the greater swelling

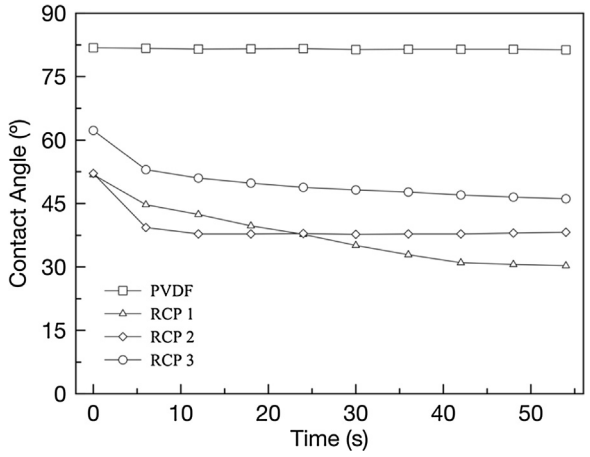

Fig. 3 – Contact angle of membranes cast from random copolymers or PVDF as a function of time.

Table 2 – Molecular weights of random copolymers and PVDF.

Polymer	M_n (g/mol)	M_w (g/mol)	Tensile strength (MPa)
RCP 1	50,000	155,000	40.1
RCP 2	26,500	82,500	–
RCP 3	25,000	84,000	42.5
PVDF	–	~534,000*	–

* Material specification from Sigma-Aldrich, measured by GPC.

softens the polymers and reduces their strength and ability to effectively bind together carbon particles. However, it is this property that can allow a greater transport of cations to the electrode pores and allow electrolyte access to pores previously blocked by the hydrophobic PVDF.

3.1.2. *Molecular weight, thermogravimetric analysis and tensile strength*

The molecular weight of the random copolymers and PVDF is presented in Table 2. The greater molecular weight of RCP 1 compared to RCP 2 and RCP 3 is a result of the greater number of sulfonic acid groups, which promotes the formation of aggregates due to hydrogen bonds between sulfonic acid groups on different polymer chains. These intermolecular forces are not thought to be as strong in the PVDF due to the presence of only hydrogen and fluorine atoms along the polymer chain. However, its greater molecular weight compared to the random copolymers is an indication of longer polymer chains and greater mechanical strength. The similarity of the molecular weights of RCP 2 and RCP 3 is a reflection of the nature of polymer synthesis, where not only monomer content but also slight differences in synthesis conditions can affect the final polymer properties, including molecular weight.

The TGA results of the three copolymers and PVDF are shown in Fig. 4.

Due to the similar compositions of all the copolymers, the family of the curves of the random copolymers exhibited similar characteristics. A small loss of absorbed ambient moisture was observed for all three copolymers, with the most obvious loss for that of the most hydrophilic copolymer RCP 1 (approximately 5% total mass loss). Three larger distinct regions of decomposition were observed for each copolymer, 250–400 °C, 400–540 °C and 540–700 °C. The two copolymers with similar molecular weights (RCP 2 and RCP 3) were seen to degrade at almost the same rate, with the greater content of the more thermally stable dihydroxydiphenyl sulfone in RCP 3 thought to have reduced the rate of degradation compared with RCP 2 in the temperature range 250–400 °C. On the other hand, despite a larger content of the less thermally stable diphenylhydroquinone monomer, the degradation of RCP 1 is seen to be less than both other copolymers. Here the monomer content appears to be less important, with the greater molecular weight of the polymer (and therefore greater intermolecular forces between the polymer chains) reducing its thermal degradation. The behaviour of PVDF was vastly different to that of the random copolymers. No ambient moisture loss was observed, and the polymer underwent rapid thermal degradation beginning at 415 °C and continuing until 470 °C, with a total mass loss of 60 wt.%. At temperatures beyond 470 °C a steady rate of mass loss was observed.

While CDI electrodes do not operate at elevated temperatures, these results reinforce the importance of chain length and molecular weight on polymer properties and in maintaining the integrity of the polymer chain. Note also that the thermal stability of the cation exchange copolymers may prove useful for fuel cell applications operating at elevated temperatures.

The tensile strengths of RCP 1 and RCP 3, shown in Table 2, were found to be 40.1 MPa and 42.5 MPa, respectively, placing both samples in the expected range for thermoplastic polymers such as PVDF, PTFE and polystyrene. The increased molecular weight of RCP 1 (on both a number-average and weight-average basis) compared to RCP 3 would normally lead one to expect RCP 1 to display a greater tensile strength than RCP 3, however this is not the case and so for this system the dominant factor is the monomer composition. Although RCP 2 was not able to yield reliable results due to defects caused during sample preparation, with a monomer ratio of dihydroxydiphenyl sulfone to diphenylhydroquinone between that of RCP 1 and RCP 3, it is reasonable to expect the tensile strength would lie somewhere between 40.1 and 42.5 MPa.

3.2. *Physical properties of carbon electrodes*

3.2.1. *Electrode thickness*

The successful formation of defect free electrodes was achieved by gentle solvent evaporation, as cracking and peeling of thin carbon films during drying can be caused by rapid solvent evaporation. Fig. 5 presents the severity of cracking that can occur due to electrode thickness, even with gentle drying conditions described in Section 2.3. Carbon electrodes composed of 75 wt.% activated carbon, 15 wt.% carbon black and 10 wt.% RCP 1 as binder were cast using a doctor blade at 200 μm, 250 μm and 300 μm. The electrode cast at

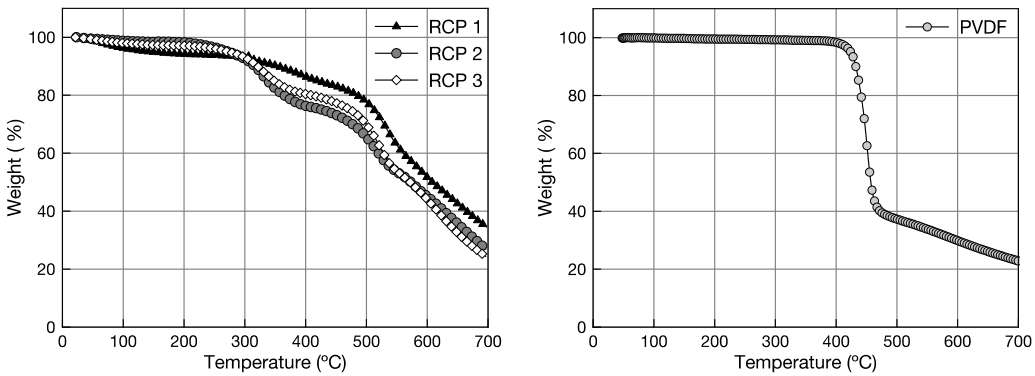

Fig. 4 – TGA results of RCP 1, RCP 2, RCP 3 and PVDF.

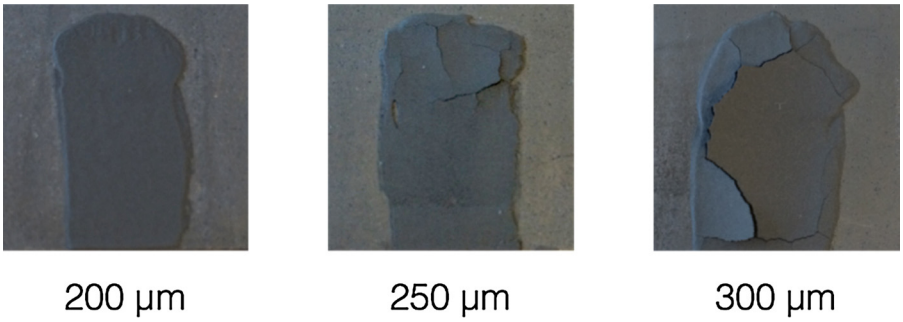

Fig. 5 – Carbon electrodes cast at 200, 250 and 300 μm, with cracks visible at thicknesses of 250 and 300 μm.

Table 3 – Contact angle of electrodes prepared with random copolymer or PVDF binder.

Binder	Contact angle (°)	Error
RCP 1	37.44	±7.38
RCP 2	36.35	±4.68
RCP 3	65.51	±1.81
PVDF	142.39	±0.05

200 μm showed no defects, however at 250 μm small cracks towards the top of the sample were visible, and at 300 μm significant cracking and peeling was observed. The thicker carbon coatings were more susceptible to cracking, as there existed both a greater quantity of solvent to evaporate and a longer, more tortuous path through which the solvent must pass.

All copolymers were repeatedly able to form defect free films cast at a thickness of 200 μm, regardless of the electrode composition or polymer used. This thickness is considered acceptable for thin film carbon electrodes (Pandolfo et al., 2010). Note that electrodes with PVDF binder were successfully cast using a doctor blade at thicknesses of 650 μm; the greater thickness of defect-free electrodes cast using PVDF highlights the additional strength of the polymer and its superior ability to bind carbon particles together.

3.2.2. *Electrode contact angle*

Table 3 presents the contact angle of the electrode fabricated from 75 wt.% activated carbon, 10 wt.% carbon black and 15 wt.% binder. All electrodes prepared with a random copolymer binder were found to have hydrophilic surfaces and contact angles much lower than electrodes prepared with a PVDF binder. RCP 1 and RCP 2 binders were observed to have similarly low contact angles, indicating very high hydrophilicity and wettability of the electrodes. In contrast, the RCP 3 electrodes were seen to have a contact angle nearly double that of the RCP 1 and RCP 2 electrodes. Such an increase between RCP 2 and RCP 3 was not expected, especially considering the similar contact angle of electrodes prepared with RCP 1 and RCP 2. This result highlights the hydrophobic effect of the dihydroxydiphenyl sulfone monomer on both the polymer and composite electrode properties, and the ability of the hydrophilic diphenylhydroquinone to increase the wettability of the electrode surface once a certain threshold has been met. In this instance, the threshold lies between a hydrophilic to hydrophobic monomer ratio of 4:6 (RCP 3) and 5:5 (RCP 2) (i.e. the ratio of diphenylhydroquinone dihydroxydiphenyl sulfone). This result also underscores the importance of polymer design when preparing polymers for specific applications such as MCDI, and the attainable improvements in wettability when using a hydrophilic binder.

Despite the variable contact angle and degree of hydrophilicity of the electrodes shown in Table 3, all electrodes fabricated with random copolymer were found to readily absorb water, as shown in Fig. 6. Over a period of 30 s, a 4 μL drop of water fully absorbed into the electrode, regardless of binder type. In contrast, the PVDF electrode's highly hydrophobic surface resulted in a very stable contact angle over the same duration.

3.2.3. *Effect of binder type and electrode composition on physical structure*

Using carbon black as a conductive filler, the amount of binder was adjusted to determine the most suitable composition. Electrodes with 5 wt.%, 10 wt.% and 15 wt.% RCP 3 were cast, each with 5 wt.% carbon black and variable activated carbon content. Electrodes with only 5 wt.% RCP 3 did not sufficiently bind and rather than forming a thin film electrode, the consistency of the samples was similar to that of the constituent powders. Although some adhesion was observed and the film was somewhat able to retain its form, when gently rinsed with water carbon was easily removed from the surface. Despite

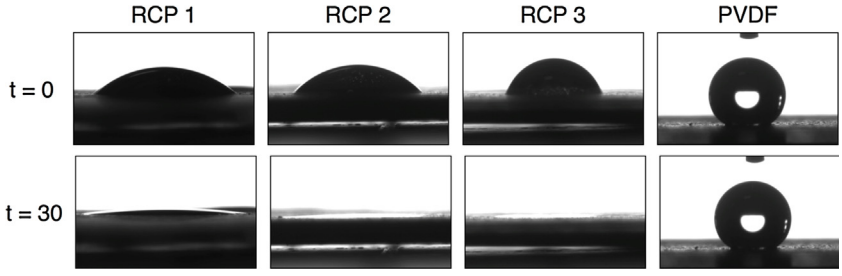

Fig. 6 – Contact angle of electrodes fabricated from 75 wt.% activated carbon, 10 wt.% carbon black and 15 wt.% binder at t = 0 s and t = 30 s.

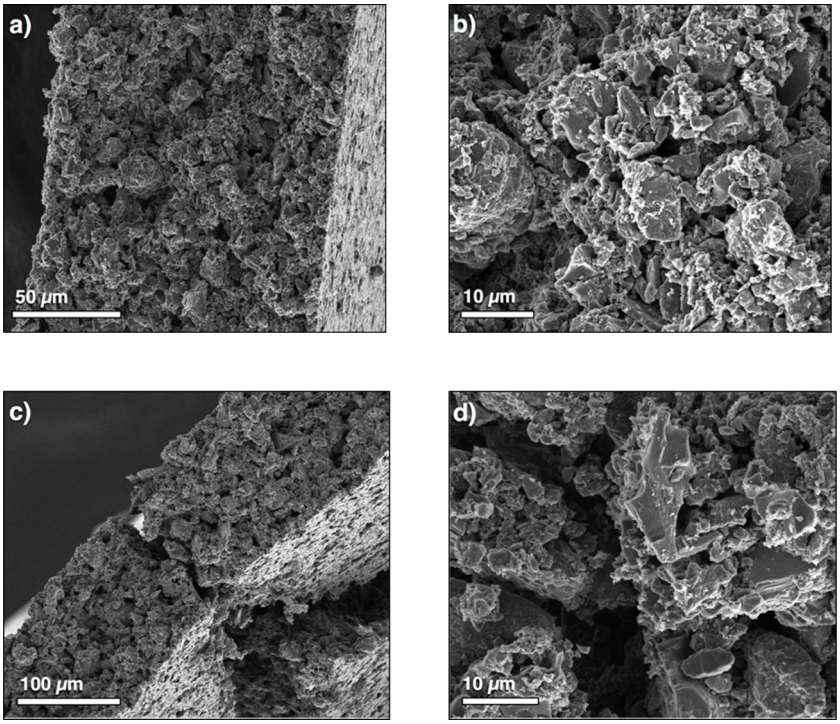

Fig. 7 – SEM images of electrodes with varying binder content: (a and b) 80 wt.% activated carbon, 5 wt.% carbon black, 15 wt.% RCP 3, (c and d) 85 wt.% activated carbon, 5 wt.% carbon black, 10 wt.% RCP 3.

ample stirring for 12–16 h to evenly disperse the polymer throughout the carbon slurry prior to casting, 5 wt.% is considered to be too low a concentration to provide adequate binding.

Electrodes prepared with 10 and 15 wt.% binder were seen to produce thin films when cast onto graphite. The 10 wt.% electrodes were found to lose a small amount of carbon during rinsing and washing, although overall the electrodes retained their form. Electrodes with 15% binder were able to retain their form and held together very well, even when soaked in water. SEM images of these electrodes can be seen in Fig. 7, with 15 wt.% binder shown in Fig. 7a and b, and 10 wt.% binder shown in Fig. 7c and d.

Samples with 15 wt.% binder were seen to form a homogeneous carbon layer free of defects, held together well by the copolymer binder. The close up SEM image in Fig. 7b reveals that good adhesion of the carbon black to the activated carbon particles was achieved. The cross-section of the 10 wt.% binder in Fig. 7c shows a large crack; although this is an artefact of the sample preparation process, it should be noted that samples with 10 wt.% binder were more difficult to handle and prepare for SEM imaging than those with 15 wt.% binder. Although the carbon particles were still well held by the binder and the carbon black adhered to the activated carbon (seen in Fig. 7d), the samples were more susceptible to breaking.

The images presented in Fig. 8 show electrodes with the same composition by mass, varying only by binder type (RCP 1, (a and b); RCP 2, (c and d); RCP 3, (e and f); PVDF, (g)). The cross-sections (Fig. 8a, c and e) reveal that regardless of binder type thin uniform electrodes were producible. From the high magnification images (Fig. 8b, d, f and g), strong adhesion of the carbon black particles to the activated carbon was observed, although no fibrils of binder connecting carbon particles could be seen. Based on these results and observations when handling the electrodes (i.e. no loss of carbon when gently rubbed), electrodes with 15 wt.% random copolymer binder (RCP 1, 2 or 3) are similar to those prepared with PVDF, and acceptable for further electrochemical characterization.

3.3. *Electrochemical characterization*

3.3.1. *Comparison of binder type using cyclic voltammetry*

The current density of electrodes prepared with RCP 1–3 or PVDF as binder material, measured using CV at scan rates of 20 mV/s and 5 mV/s, is shown in Figs. 9 and 10. The electrodes consisted of 75 wt.% activated carbon, 10 wt.% graphite and 15 wt.% binder.

Samples prepared with copolymer binder were observed to form rectangular curves at 20 mV/s (Fig. 9), which is a typical response for carbon/polymer composite electrodes (Tian et al., 2014; Wang et al., 2014). In contrast, samples with PVDF binder produced larger, more distorted curves typical of electrodes at a fast scan rate with negligible micropore penetration. At a slower scan rate of 5 mV/s (Fig. 10), the PVDF samples produced more rectangular curves with an increased current density over the 20 mV/s scan, indicating double layer formation within the micropores. For samples prepared with the random copolymers, no changes in shape were observed between the two scan rates, and the current density only decreased proportionately to the change in scan rate. This indicates the electrodes had almost reached their maximum electrosorption capacity and that negligible micropore penetration was occurring, even at a slower scan rate. Thus, the random copolymer binders appeared to facilitate double layer formation in the mesopores while restricting micropore double layer formation.

The low current density of electrodes prepared with random copolymer binders is expected to be a result of either poor electrode conductivity or poor ionic conductivity. The hydrophilic nature of the random copolymers suggests that sufficient ion mobility can be achieved, with the potential for the random copolymers to even increase capacitance by

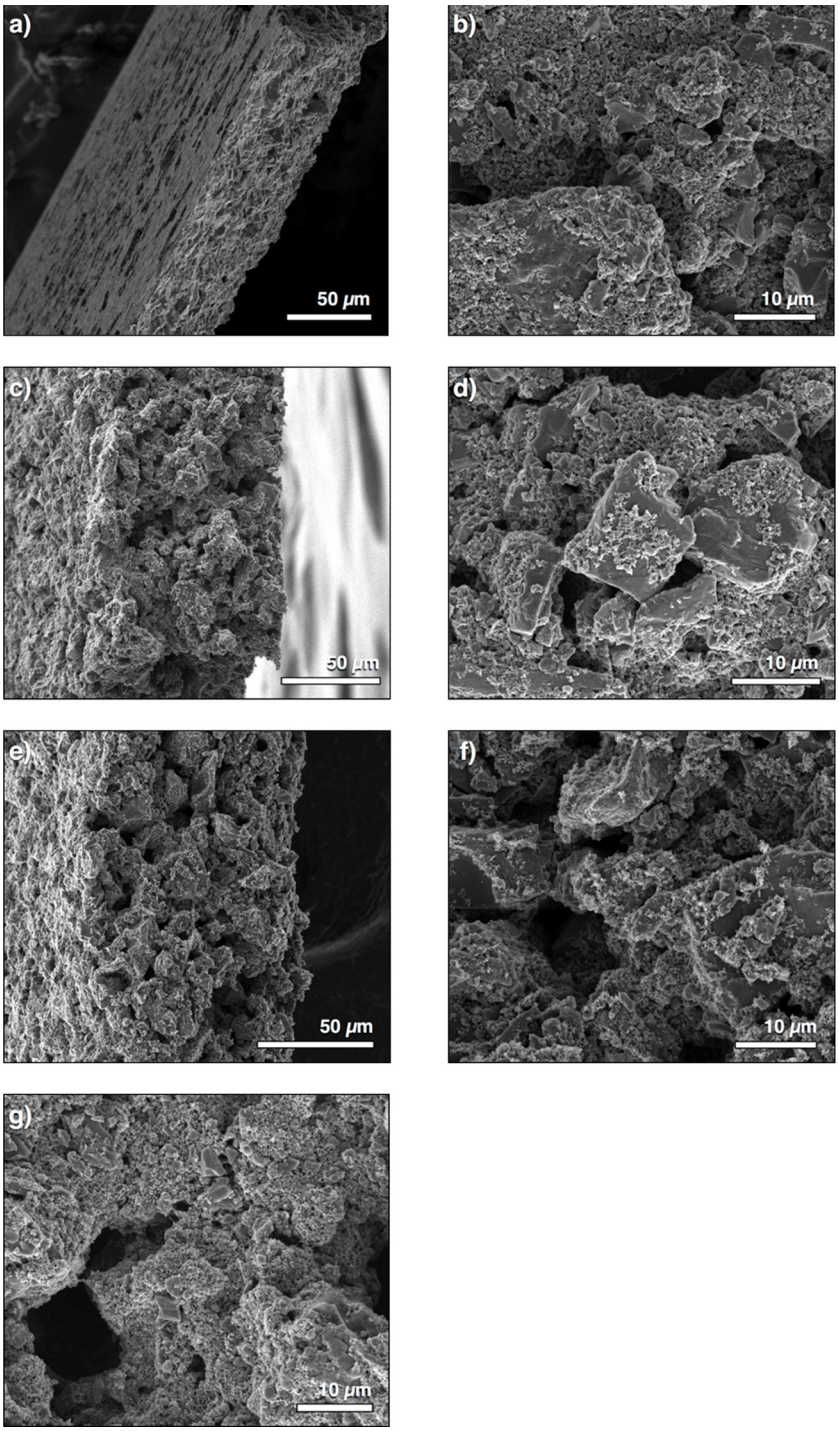

Fig. 8 – Cross-section and surface SEM images of electrodes consisting of 75 wt.% activated carbon, 10 wt.% carbon black and 15 wt.% polymer binder, prepared with the following binders: (a and b) RCP 1, (c and d) RCP 2, (e and f) RCP 3, (g) PVDF (surface only).

allowing electrolyte transport to previously blocked pores. The low capacitance is therefore likely due to poor electrode conductivity, reducing the carbon's ability to form microporous double layers. It is postulated that this is due to a loss of charge transfer pathways between the carbon particles, caused by the swollen random copolymer, as demonstrated in Fig. 11. The hydrophobic PVDF binder does not swell in solution and allows carbon particles to remain in contact with both each other and with carbon black particles. In contrast, the hydrophilic copolymer swells to a much greater degree and causes some of this contact to be lost, meaning particles further away from the current collector are less conductive. This is represented by the shading of the particles in Fig. 11, where a lower conductivity is represented by lighter coloured particles. Although the polymers are conductive and do allow some charge transfer, this is not as great as direct particle contact.

Note also that the tests were conducted in 0.5 M NaCl, while practical applications of CDI involve the desalination of brackish water which is considerably less conductive. This should serve to reduce the conductivity of the electrolyte solution within the swollen polymers and decrease the transfer of charge between particles even further.

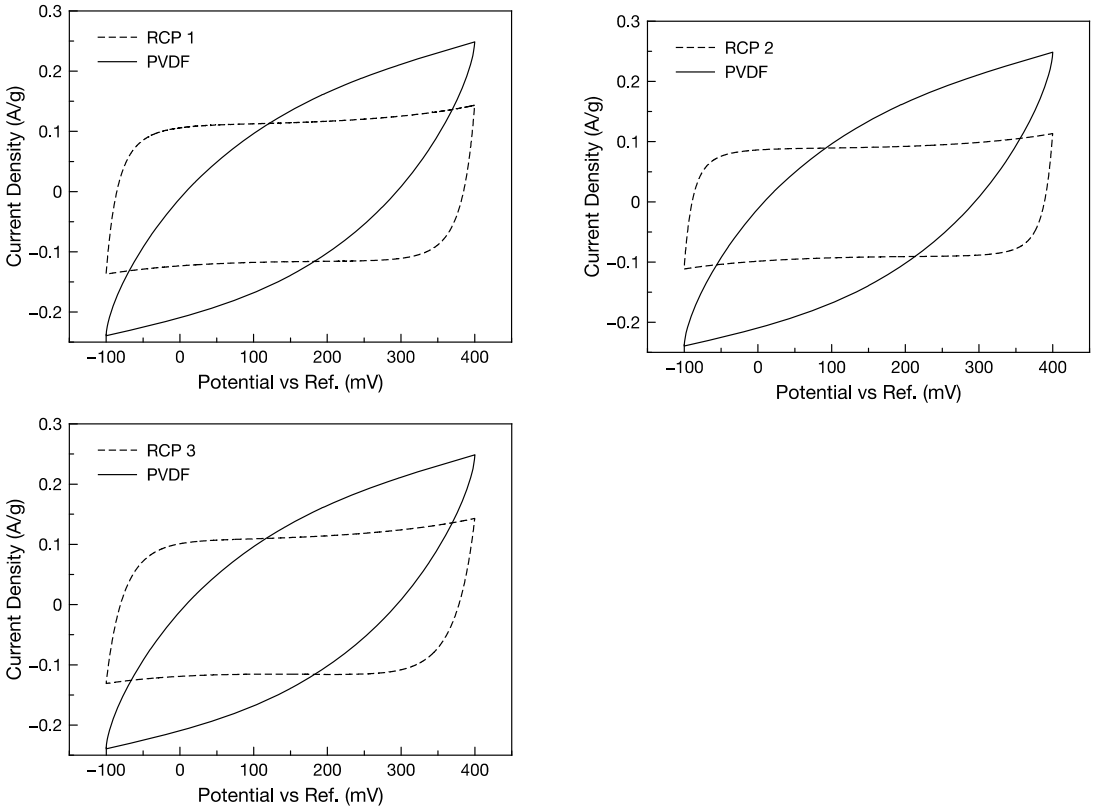

Fig. 9 – Current density of electrodes with various polymers used as binders, measured at 20 mV/s in 0.5 M NaCl.

3.3.2. *Electrochemical impedance spectroscopy*

The Nyquist plots of the electrodes are presented in Fig. 12. Similarly to the CV curves, different responses caused by the binder type (PVDF or random copolymer) were observed. The shape of all curves was typical for that of a double layer capacitor, notwithstanding the large magnitude of the imaginary impedance for the random copolymers, nor the large real and imaginary impedances for the PVDF binder.

PVDF electrodes showed very large charging resistance at low frequencies, which is highlighted in Fig. 13. Conversely, the copolymer binder electrodes had much lower resistance, with the real impedance only increasing notably at frequencies

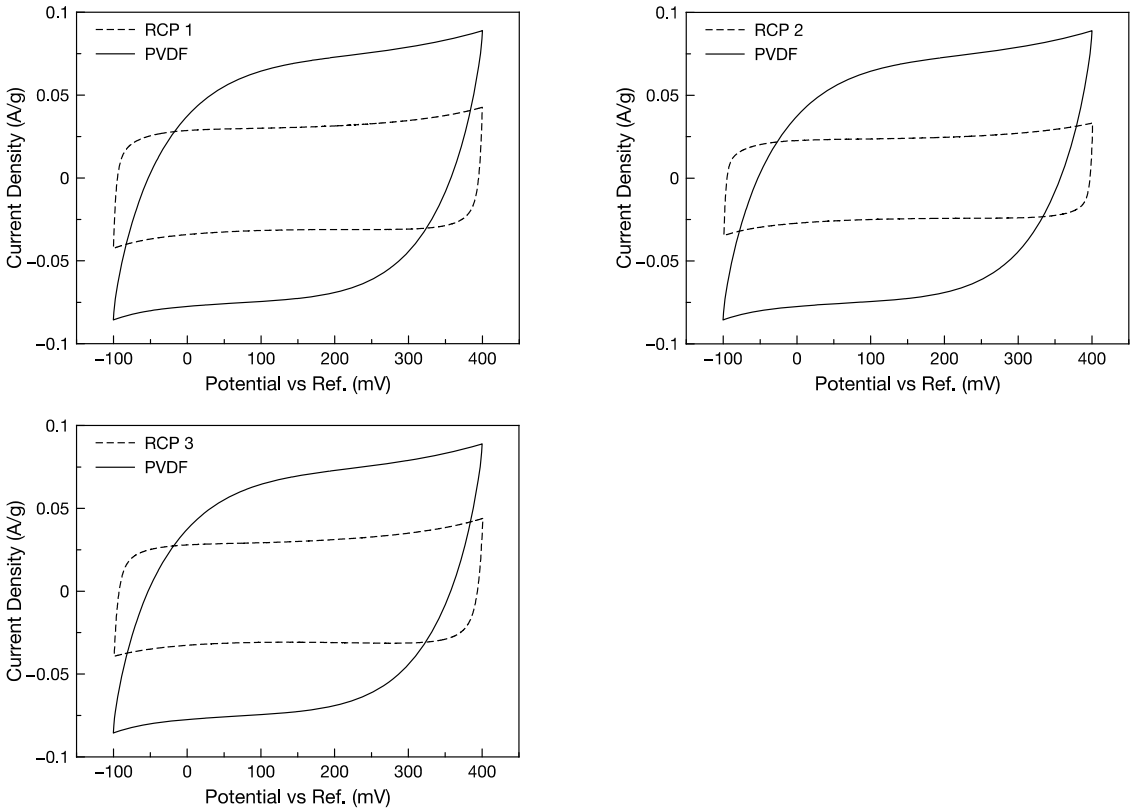

Fig. 10 – Current density of electrodes with various polymers used as binders, measured at 5 mV/s in 0.5 M NaCl.

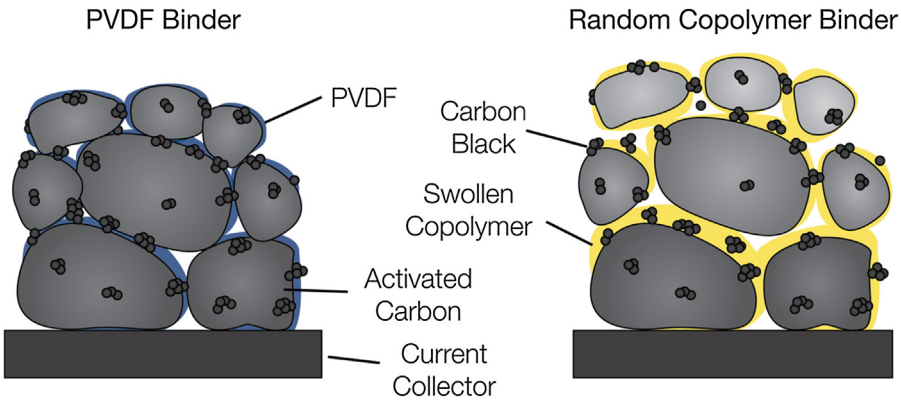

Fig. 11 – Illustration of the potential loss of charge transfer pathways within a carbon electrode using a hydrophilic binder. Carbon electrodes prepared with PVDF (left) remain in contact with each other, while the swollen random copolymer (right) reduces particle contact and hence conductivity. Darker particles represent those that have a greater conductivity.

lower than 100 mHz. This may be a combination of minimal micropore penetration as well as the ability of the copolymers to facilitate electrolyte transport. The low resistance at high frequencies, combined with the increase in capacitance at high frequencies compared with the PVDF (shown in Fig. 14), suggests that the random copolymers facilitate fast mesopore double layer formation, despite the swelling reducing the micropore capacitance.

The differences in capacitance for electrodes with different random copolymer binders were seen to follow the trend of lower swelling yielding greater capacitance, such that the capacitance of the electrodes with RCP 3 binder > RCP 2 binder > RCP 1 binder. The reduced swelling of RCP 3 allows better particle contact, more charge transfer pathways and greater electrode conductivity, despite the polymer itself having a lower conductivity. Considering the highly microporous nature of the activated carbon used in this study, a significant proportion of the surface area is inaccessible with a large proportion of pore openings below the cut-off width. Thus, capacitances that exceeds that of PVDF binder electrodes might be observed when using these copolymers as binders in electrodes fabricated from carbons with a higher proportion of mesopores and large micropores, such as ordered mesoporous carbon.

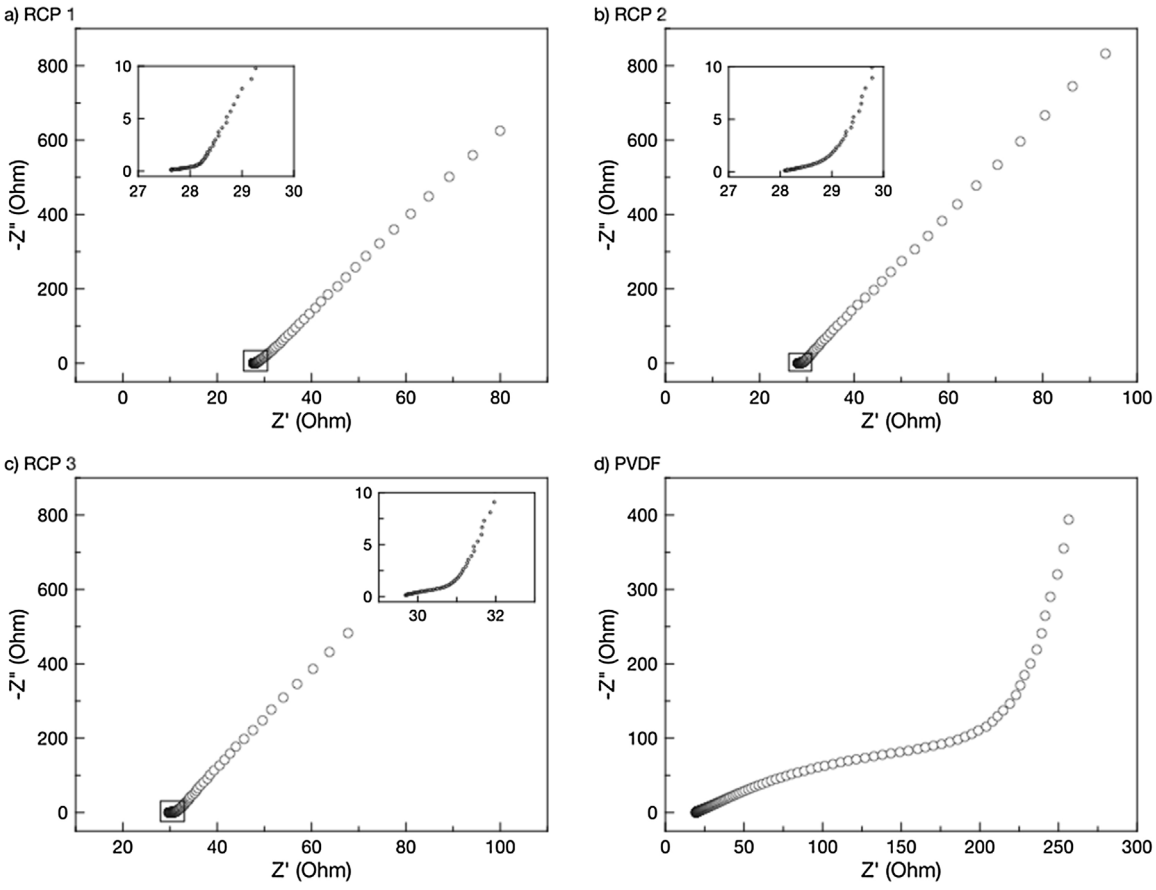

Fig. 12 – Nyquist plots of electrodes with 15 wt.% binder: (a) RCP 1, (b) RCP 2, (c) RCP 3 and (d) PVDF.

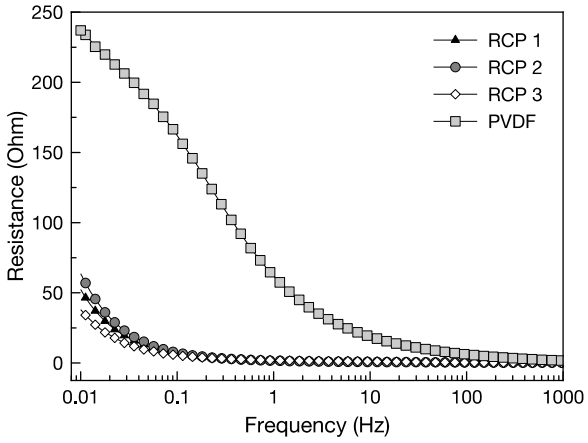

Fig. 13 – Resistance versus frequency of electrodes with various binder materials.

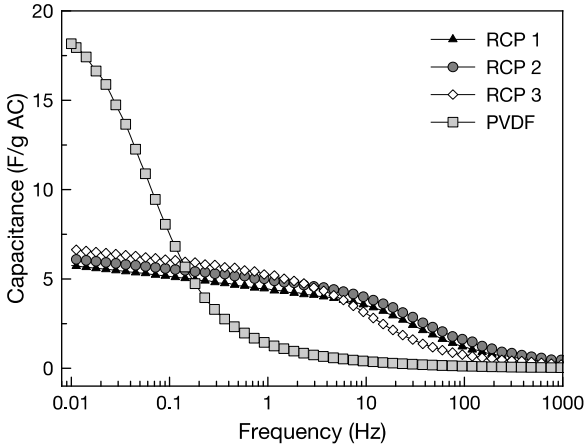

Fig. 14 – Capacitance versus frequency of electrodes with various binder materials.

4. Conclusions

Carbon electrodes were prepared with random poly(arylene ether sulfone)s as binder materials and compared with those prepared with PVDF as a binder. A copolymer mass composition of 15% was found to adequately bind carbon particles, with no loss of carbon observed when treated in water. Regardless of the polymer used, good adhesion of the conductive carbon black to the activated carbon was observed. Electrodes with 10 wt.% random copolymer, while still forming thin carbon layers, were more brittle and lost some carbon when treated with water, and those with 5 wt.% random copolymer provided no effective binding. The maximum thickness of electrodes prepared with the random copolymers was lower than those prepared with PVDF, and although an acceptable casting thickness of 200 μm was achieved, this result highlighted the loss in strength when the copolymers were used.

The hydrophilic copolymers were observed to have low contact angles and swelling rates in the range of 26.4–49.9%. The effect of this hydrophilicity was directly observed when the random copolymers were incorporated into carbon electrodes. Electrode surfaces were observed to be hydrophilic with low contact angles in the range of 37.44–65.51° and readily absorbed water. In comparison, electrodes prepared with a PVDF binder were hydrophobic with a contact angle of 142.39°, and no absorption of water into the electrode was observed.

CV and EIS testing revealed that although the binders improved wettability and were able to provide adequate strength at 15 wt.%, the capacitance of the electrodes was lower than electrodes prepared with PVDF. The high swelling rates of the polymers are thought to have reduced the charge transfer pathways between carbon particles, resulting in a lack of micropore double layer formation. The increases in capacitance at high EIS frequencies and lower charging resistance suggested that a more hydrophobic polymer that can facilitate the selective transport of ions better than PVDF, and may indeed yield greater conductivities by maintaining charge transfer pathways. Furthermore, the use of an activated carbon material with larger micropores and a greater mesoporous surface area may improve results such that they are comparable or even exceed those achieved with a hydrophobic binder such as PVDF. Further work on this topic should include assessing the CDI desalination performance of electrodes with copolymer binders.

Acknowledgements

The authors acknowledge the financial support of the National Centre of Excellence in Desalination Australia, which is funded by the Australian Government through the Water for the Future Initiative. Benjamin Asquith acknowledges the financial support of the German Academic Exchange Service (DAAD), which supported his visit to IPF Dresden.

References

Asquith, B.M., Meier-Haack, J., Ladewig, B.P., 2014. Cation exchange copolymer enhanced electrosorption. Desalination 345, 94–100.

Asquith, B.M., Meier-Haack, J., Vogel, C., Butwilowski, W., Ladewig, B.P., 2013. Side-chain sulfonated copolymer cation exchange membranes for electro-driven desalination applications. Desalination 324, 93–98.

Bouhadana, Y., Avraham, E., Noked, M., Ben-Tzion, M., Soffer, A., Aurbach, D., 2011. Capacitive deionization of NaCl solutions at non-steady-state conditions: inversion functionality of the carbon electrodes. J. Phys. Chem. C 115, 16567–16573.

Chang, L., Yu, Y., Duan, X., Liu, W., 2012. Capacitive deionization performance of activated carbon electrodes prepared by a novel liquid binder. Sep. Sci. Technol. (Philadelphia) 48, 359–365.

Choi, J.H., 2010. Fabrication of a carbon electrode using activated carbon powder and application to the capacitive deionization process. Sep. Purif. Technol. 70, 362–366.

El-Deen, A.G., Barakat, N.A.M., Khalil, K.A., Kim, H.Y., 2014. Hollow carbon nanofibers as an effective electrode for brackish water desalination using the capacitive deionization process. New J. Chem. 38, 198–205.

Farmer, J.C., 1995. Method and Apparatus for Capacitive Deionization, Electrochemical Purification, and Regeneration of Electrodes, in: US Patent (Ed.).

Hou, C.H., Huang, C.Y., 2013. A comparative study of electrosorption selectivity of ions by activated carbon electrodes in capacitive deionization. Desalination 314, 124–129.

Hou, C.H., Huang, J.F., Lin, H.R., Wang, B.Y., 2012. Preparation of activated carbon sheet electrode assisted electrosorption process. J. Taiwan Inst. Chem. Eng. 43, 473–479.

Huang, Z.H., Wang, M., Wang, L., Kang, F., 2012. Relation between the charge efficiency of activated carbon fiber and its desalination performance. Langmuir 28, 5079–5084.

Jande, Y.A.C., Kim, W.S., 2014. Integrating reverse electrodialysis with constant current operating capacitive deionization. J. Environ. Manage. 146, 463–469.

Jande, Y.A.C., Minhas, M.B., Kim, W.S., 2013. Ultrapure water from seawater using integrated reverse osmosis-capacitive deionization system. Desalin. Water Treat. 53 (13), 3482–3490.

Kim, Y.J., Choi, J.H., 2010. Desalination of brackish water by capacitive deionization system combined with ion-exchange membrane. Appl. Chem. Eng. 21, 87–92.
Lee, J.B., Park, K.K., Yoon, S.W., Park, P.Y., Park, K.I., Lee, C.W., 2009. Desalination performance of a carbon-based composite electrode. Desalination 237, 155–161.
Lee, J.H., Choi, J.H., 2012. The production of ultrapure water by membrane capacitive deionization (MCDI) technology. J. Membr. Sci. 409–410, 251–256.
Li, H., Zou, L., 2011. Ion-exchange membrane capacitive deionization: a new strategy for brackish water desalination. Desalination 275, 62–66.
Mossad, M., Zhang, W., Zou, L., 2013. Using capacitive deionisation for inland brackish groundwater desalination in a remote location. Desalination 308, 154–160.
Mossad, M., Zou, L., 2012. A study of the capacitive deionisation performance under various operational conditions. J. Hazard. Mater. 213–214, 491–497.
Mossad, M., Zou, L., 2013. Evaluation of the salt removal efficiency of capacitive deionisation: kinetics, isotherms and thermodynamics. Chem. Eng. J. 223, 704–713.
Nie, C., Pan, L., Liu, Y., Li, H., Chen, T., Lu, T., Sun, Z., 2012. Electrophoretic deposition of carbon nanotubes-polyacrylic acid composite film electrode for capacitive deionization. Electrochim. Acta 66, 106–109.
Pandolfo, A.G., Wilson, G.J., Huynh, T.D., Hollenkamp, A.F., 2010. The influence of conductive additives and inter-particle voids in carbon EDLC electrodes. Fuel Cells 10, 856–864.
Park, B.H., Choi, J.H., 2010. Improvement in the capacitance of a carbon electrode prepared using water-soluble polymer binder for a capacitive deionization application. Electrochim. Acta 55, 2888–2893.
Park, B.H., Kim, Y.J., Park, J.S., Choi, J., 2011. Capacitive deionization using a carbon electrode prepared with water-soluble poly(vinyl alcohol) binder. J. Ind. Eng. Chem. 17, 717–722.
Porada, S., Bryjak, M., Van Der Wal, A., Biesheuvel, P.M., 2012. Effect of electrode thickness variation on operation of capacitive deionization. Electrochim. Acta 75, 148–156.
Ryoo, M.W., Kim, J.H., Seo, G., 2003. Role of titania incorporated on activated carbon cloth for capacitive deionization of NaCl solution. J. Colloid Interface Sci. 264, 414–419.
Ryoo, M.W., Seo, G., 2003. Improvement in capacitive deionization function of activated carbon cloth by titania modification. Water Res. 37, 1527–1534.
Tian, G., Liu, L., Meng, Q., Cao, B., 2014. Preparation and characterization of cross-linked quaternised polyvinyl alcohol membrane/activated carbon composite electrode for membrane capacitive deionization. Desalination 354, 107–115.
Villar, I., Roldan, S., Ruiz, V., Granda, M., Blanco, C., Menéndez, R., Santamaría, R., 2010. Capacitive deionization of NaCl solutions with modified activated carbon electrodes. Energy Fuels 24, 3329–3333.
Vogel, C., Komber, H., Quetschke, A., Butwilowski, W., Pötschke, A., Schlenstedt, K., Meier-Haack, J., 2011. Side-chain sulfonated random and multiblock poly(ether sulfone)s for PEM applications. React. Funct. Polym. 71, 828–842.
Wang, G., Pan, C., Wang, L., Dong, Q., Yu, C., Zhao, Z., Qiu, J., 2012. Activated carbon nanofiber webs made by electrospinning for capacitive deionization. Electrochim. Acta 69, 65–70.
Wang, G., Qian, B., Dong, Q., Yang, J., Zhao, Z., Qiu, J., 2013. Highly mesoporous activated carbon electrode for capacitive deionization. Sep. Purif. Technol. 103, 216–221.
Wang, Y., Zhang, L., Wu, Y., Xu, S., Wang, J., 2014. Polypyrrole/carbon nanotube composites as cathode material for performance enhancing of capacitive deionization technology. Desalination 354, 62–67.
Xu, P., Drewes, J.E., Heil, D., Wang, G., 2008. Treatment of brackish produced water using carbon aerogel-based capacitive deionization technology. Water Res. 42, 2605–2617.
Zhang, W., Mossad, M., Zou, L., 2013. A study of the long-term operation of capacitive deionisation in inland brackish water desalination. Desalination 320, 80–85.
Zhang, Y., Guo, J., Li, T., 2012. Research progress on binder of activated carbon electrode. Adv. Mater. Res., 780–784.